

# VISCOELASTICITY OF POLYETHYLENES PRODUCED WITH SINGLE SITE METALLOCENE CATALYSIS

*Esra Kucukpinar, Dilhan M. Kalyon, Paul. P. Tong  
Highly Filled Materials Institute  
Stevens Institute of Technology  
Castle Point, Hoboken, NJ*

## Abstract

Linear low density polyethylene (LLDPE) produced using metallocene catalysts is gaining prominence as a class of new polyethylenes with superior performance. Two recently commercialized metallocene-catalyzed linear low density polyethylene resins were characterized in terms of their storage and loss moduli, shear viscosity, shear stress growth, stress relaxation upon cessation of steady shear, and first normal stress difference material functions. Overall the rheological behavior reflects the relatively narrow molecular weight distributions of the resins. The oscillatory shear and relaxation moduli data were employed to determine the parameters of Wagner model. Various material functions, determined on the basis of this model in conjunction with the fitted parameters, agreed reasonably well with the experimental results. The reported data and parameters should facilitate an improved understanding of the processability characteristics of these two new LLDPEs.

## Introduction

After initial commercialization in the 1940's, polyethylene has evolved into one of the most important class of thermoplastic resins. In recent years, there has been an enormous growth in the work related to a new class of catalyst for olefin polymerization, the metallocene catalysts. The key advantage of such catalysts is the precise tailoring of molecular characteristics. The molecular weight distributions (MWD) are generally narrow, with improvements in the control of distributions of short chain branching (SCB) and long chain branching (LCB) in the polymer [1 & 2]. Only a few papers have been published on the rheology of this new class of polyethylenes. Chien *et al* [3] have worked on the dynamic viscoelastic measurements of polypropylenes obtained via ansa-metallocene catalyst systems. Vega *et al* [4] have studied the linear viscoelastic and steady state flow properties of a series of metallocene-catalyzed polyethylenes.

In this study, a broad-based experimental program has been conducted to extensively characterize the rheological behavior of two commercially available

metallocene-catalyzed LLDPE. The various material functions studied include storage and loss moduli, relaxation modulus, shear viscosity and first normal stress difference. The behavior of these materials is interpreted in terms of integral type nonlinear models. We use dynamic measurements to characterize the linear viscoelasticity, and step-shear experiments to elucidate the non-linear response. These, cast in the framework of the integral constitutive equation, allow the prediction of other material functions, which can be checked with experiments. The rheological constitutive equation thus validated will allow the modelling of complex processing flows for this important new class of resins.

## Experimental

**Materials.** In this study two different types of commercially available metallocene LLDPE were used. Both are hexene copolymers produced using Exxon Chemical's EXXPOL technology. Exceed 350D60 is a tough premium film resin, while 357C80, is a premium cast stretch film resin. Films made from these resins have been reported to have outstanding tensile, impact and puncture toughness. In [Table 1](#) some general properties of the two resins are presented. The two resins have similar polydispersity.

**Rheology.** Most of the rheological characterization was carried out using a Rheometrics Mechanical Spectrometer System IV. A new ARES rheometer system made by Rheometric Scientific was also used as a spot check. Samples were premolded at 180 °C. Parallel plate geometry was used for the dynamic and step shear experiments. In the large strain experiments, correction for non-homogeneous strain for the parallel plate geometry was applied [5]. Steady shear experiments were carried out employing the cone and plate fixtures. These include stress growth at start-up of steady shear and stress relaxation after cessation of steady shear. The cone diameter and angle were 25 mm. and 0.1 rad (5.72 °), respectively. The cone-and-plate geometry was necessary to assure a uniform strain rate distribution in the radial direction. The shear viscosity of the two polyethylenes at the higher shear rate range of 10 to 1000 s<sup>-1</sup> was also measured by using an Instron Capillary Rheometer. The

capillary aspect ratio was  $L/D=40$  at diameters of 1.27, 1.524 and 1.778 mm. True shear viscosity values were obtained using the standard Bagley and Rabinowitsch corrections (see, for example J. Dealy [6]).

Constitutive Equation.

The following integral K-BKZ type, network-based constitutive equation is used,

$$\tau = \int_{-\infty}^t [M_1(s, I_1, I_2) \mathbf{B}] ds \quad (1)$$

where  $s$  is the elapsed time, i.e.,  $t-t'$ , where  $t$  is the present time. The memory function  $M_1$  is assumed to be functions of the time differences and the first,  $I_1$ , and second,  $I_2$  invariants of the Finger tensor  $\mathbf{B}$ . [7].  $M_1$  is expressible as a product of two functions, [8]

$$M_1(s, I_1, I_2) = M_0(s) h(I_1, I_2) \quad (2)$$

where  $h(I_1, I_2) \leq 1$  is called the damping function. It tends to one for small deformations and  $M_0(s)$  is identical with the rubberlike-liquid memory function, as determined from linear viscoelastic data. In this study,

$$M_0(s) = \sum_i \frac{G_{oi}}{\lambda_i} \exp\left(-\frac{t-t'}{\lambda_i}\right) \quad (3)$$

is chosen where the  $G_{oi}$  and  $\lambda_i$  are the relaxation strength and time, respectively.

For shear flow, the damping function used in this study has a double exponential dependence to strain [9]:

$$h(\gamma) = f \exp(-n_1\gamma) + (1-f) \exp(-n_2\gamma) \quad (3a)$$

where  $f$ ,  $n_1$ ,  $n_2$  are material parameters.

Various material functions predicted on the basis of the constitutive equation are given in Table (2). These can be determined by closed integration. The predicted material functions, valid at the reference temperature of  $T_o = 180$  °C, were compared with the experimental measurements and the comparisons are discussed.

## Results and Discussion

To determine the linear viscoelastic region of the melts, strain sweep experiments were carried out in the strain amplitude range between 1 and 400% at a frequency of 1 rad/s for both of the LLDPE's. The results indicate that the dynamic properties  $G'$  and  $G''$  are independent of strain, thus behaving as a linear viscoelastic material over a broad strain amplitude range, up to >100%. The frequency dependence of the dynamic properties were characterized at the strain amplitude of 15 %.

The storage and loss moduli of the resin 350D60 are shown in Figures 1. The frequency range was broadened by using the time temperature superposition principle. Data were collected at temperatures of 160, 180 and 200 °C, and then shifted to the reference temperature of 180

°C. As shown, good superposition is obtained. From the shift factors, the flow activation energy was determined to be 7.4 Kcal/mole, which is consistent with literature values for LLDPE. The dynamic moduli curves for the two resins have similar shapes, but shifted in frequency. This is consistent with the fact that they are similar MWD, differing only in MW.

From the dynamic data, the discrete relaxation spectra for the two resins were determined employing a pattern search method which minimizes the objective function,  $F$  defined

$$as: F = \sum_{i=1}^N [((G'_{i,exp} - G'_{i,fit})/G'_{i,exp})^2 + ((G''_{i,exp} - G''_{i,fit})/G''_{i,exp})^2]$$

where  $N$  is the number of data points,  $(G'_{i,exp}, G''_{i,exp})$  available from the dynamic experiments and  $G'_{i,fit}$  and  $G''_{i,fit}$  denote the best fit values on the basis of Equation (5) and (6) from Table 2. The low-frequency behavior is dominated by the long relaxation times and the high-frequency response is controlled by the short relaxation times [10]. This representation makes it possible to describe the linear viscoelastic behavior over a wide range of time values by means of only a few constants [11]. The relaxation strengths  $G_{oi}$  represent the contribution to rigidity associated with relaxation times which lie in the interval  $\ln \lambda$  and  $\ln \lambda + d \ln \lambda$ , are listed in Table 3.

TABLE 3: Relaxation Time  $\lambda_i$  and Strength  $G_{oi}$

|                | Exceed 357C80 | Exceed 350D60 |
|----------------|---------------|---------------|
| $\lambda_i, s$ | $G_{oi}, Pa$  | $G_{oi}, Pa$  |
| 10             | 8.00E+00      | 1.94E+01      |
| 1              | 5.00E+01      | 8.33E+02      |
| 0.1            | 5.14E+03      | 3.93E+04      |
| 0.01           | 1.42E+05      | 3.48E+05      |
| 0.001          | 2.00E+05      | 3.70E+05      |
| 0.0001         | 3.96E+06      | 1.00E+06      |

The results of the step - strain experiments are shown in Fig. 2, after correction for inhomogeneous strain in the parallel plate geometry. Data from 50 to 900% were shown. At strains higher than 100%, the relaxation modulus shows clear dependence on strain, and hence non-linear behavior. At low strains, in the linear viscoelastic region, the shear relaxation modulus values can be calculated from the relaxation spectrum through:

$$G(t) = \sum_i G_{oi} \exp(-t/\lambda_i) \quad (4)$$

The prediction is indicated by the solid curve in Figures 3. The agreement is good, and provides support to the relaxation spectrum obtained from the dynamic data.

At higher strains, in the non-linear region, the relaxation modulus curves are essentially parallel to one another, superposable by a vertical shift. Thus the relaxation behavior is separable into a time-dependent modulus and

a strain dependent damping function,  $h(\gamma)$ , according to eq. 2. The damping function is given by the vertical shift required to superimpose the curves at various strains onto the reference curve representing the linear viscoelastic region. The parameters from fitting to eq. 3a are shown below in Table 4, which can now be used to predict other material functions.

TABLE 4: Parameters in Double Exponential Damping Function

|    | PE-350 | PE-357 |
|----|--------|--------|
| f  | 0.16   | 0.72   |
| n1 | 0.01   | 0.12   |
| n2 | 0.22   | 0.38   |

For the start - up flow experiments, Fig. 3 shows the experimental shear stress growth behavior versus the predictions of the Wagner model (Table 2, Eq. 9). Here data from the newer ARES rheometer are also available for comparison. Overall, the agreement is acceptable, and the ARES data are closer to the model prediction. The model prediction for the growth of the first normal stress difference is also reasonable in view of the increased scatter in the normal stress data.

The predicted shear viscosity values of the materials are compared to the experimental values determined with cone and plate flow at 180 °C in Fig. 4. Included for comparison are high shear rate data from capillary rheometry and the magnitude of the complex viscosity. According to the well-known empirical Cox - Merz relationship (see, for example, Bird *et al* [10]), the magnitude of the complex viscosity approaches the shear viscosity at corresponding values of shear rate and frequency. The experimental results compare well with the model prediction.

Next, we study the stress relaxation behavior after cessation of steady shear. The comparison of experimental and predicted shear stress relaxations is shown in Fig. 5. Again the overall agreement between the experimental and predicted relaxation values is satisfactory.

## Conclusions

Various viscoelastic material functions of two metallocene catalyzed linear low density polyethylenes were characterized. The K-BKZ model (Wagner's

Postulate) was used to best fit the dynamic and relaxation modulus data, through the relaxation spectrum and damping function. The fitted parameters then allow prediction other material functions. The agreement between the model predictions and experimental data was generally acceptable. Compared to resin 357C80, resin 350D60 had higher viscosity, first normal stress difference, as well as high dynamic moduli and relaxation modulus. These are all consistent with the difference in molecular weight, as well as the similarity in molecular weight distribution for the two resins. The data and the K-BKZ parameters can be employed to predict the processing behavior of these two commercial metallocene resins in various extrusion and molding flows.

## Acknowledgements

We thank Dr. Garcia-Franco & Exxon Corporation for the materials and data in Table 1, and Mr. H. Gevgilili for help in experimental work.

## References

- Schwank D., Mod. Plast. Int., 40-41 [1983].
- Garbassi F., Gila L., Proto A., Polym. News 19, 367-371 [1984]
- Chien J. C. W., Linas G. H., Rausch M. D., Lin Y. G., Winter H. H., Atwood T. L., Bott S. C., J Polym. Sci., Part A Polym. Chem. 30, 2601-2617 [1992].
- Vega Munoz-Escalona, Santa Maria, A. Munoz, M. E., LaFuenta, P., Macromolecules, 29, 960-965 [1996].
- Soskey P., Winter H., J. Rheol., 28, 5, 625 [1984].
- Dealy J., Rheometers for Molten Plastics, Van Nostrand Reinhold, New York [1982].
- Wagner M. H., Rheol. Acta, 16, 43-50 [1977].
- Wagner M. H., Rheol. Acta, 16, 133 [1976].
- Osaki K., Proc. VII th Int Congr. Rheology, 104, (Gothenburg, Sweden) [1976].
- Bird, R. B., Armstrong, R. C. and Hassager, O., "Dynamics of Polymeric Liquids, Volume I, Fluid Mechanics", John Wiley and Sons, New York [1977].
- Laun H. M., Rheol. Acta, 17, 1 [1978].
- Wagner M. H., Rheol. Acta, 15, 136 [1976].
- Kalyon D., Yu D and Yu J, J. Rheol, 789 [1988]

TABLE 1: Properties of Metallocene-Catalyzed Linear Low Density Polyethylene Resins

|               | $M_w$<br>(g/mol) | $M_w/M_n$ | Melt Index<br>(g/10 min) | Density<br>(g/cm <sup>3</sup> ) | Melting Point<br>°F (°C) |
|---------------|------------------|-----------|--------------------------|---------------------------------|--------------------------|
| <b>350D60</b> | 100000           | 2.5       | 1                        | 0.917                           | 246(119)                 |
| <b>357C80</b> | 80000            | 2.5       | 3.4                      | 0.917                           | 239(115)                 |

**TABLE 2: Various Shear Material Functions According to Wagner Model<sup>(a)</sup>**

**Small Amplitude Oscillatory Shear Flow**

$$G'(\omega) = \sum_i \frac{G_{oi} \lambda_i^2 \omega^2}{1 + \lambda_i^2 \omega^2} \quad (5)$$

$$G''(\omega) = \sum_i \frac{G_{oi} \lambda_i \omega}{1 + \lambda_i^2 \omega^2} \quad (6)$$

**Steady - Shear Flow**

$$\eta(\dot{\gamma}) = f \sum_i \frac{G_{oi} \lambda_i}{(1 + n_1 \dot{\gamma} \lambda_i)^2} + (1-f) \sum_i \frac{G_{oi} \lambda_i}{(1 + n_2 \dot{\gamma} \lambda_i)^2} \quad (7)$$

$$\psi_1(\dot{\gamma}) = f \sum_i \frac{2G_{oi} \lambda_i^2}{(1 + n_1 \dot{\gamma} \lambda_i)^3} + (1-f) \sum_i \frac{2G_{oi} \lambda_i^2}{(1 + n_2 \dot{\gamma} \lambda_i)^3} \quad (8)$$

**Start - up Flow**

$$\eta^+(t, \dot{\gamma}) = f \sum_i \frac{G_{oi} \lambda_i}{(1 + n_1 \dot{\gamma} \lambda_i)^2} [1 - \exp(-t_{1,i})(1 - n_1 \dot{\gamma} \lambda_i t_{1,i})] + (1-f) \sum_i \frac{G_{oi} \lambda_i}{(1 + n_2 \dot{\gamma} \lambda_i)^2} [1 - \exp(-t_{2,i})(1 - n_2 \dot{\gamma} \lambda_i t_{2,i})] \quad (9)$$

$$\psi_1^+(t, \dot{\gamma}) = f \sum_i \frac{2G_{oi} \lambda_i^2}{(1 + n_1 \dot{\gamma} \lambda_i)^3} [1 - \exp(-t_{1,i})(1 + t_{1,i} - \frac{n_1 \dot{\gamma} \lambda_i}{2} t_{1,i}^2)] + (1-f) \sum_i \frac{2G_{oi} \lambda_i^2}{(1 + n_2 \dot{\gamma} \lambda_i)^3} [1 - \exp(-t_{2,i})(1 + t_{2,i} - \frac{n_2 \dot{\gamma} \lambda_i}{2} t_{2,i}^2)] \quad (10)$$

$$\text{where } t_{1,i} = \frac{1 + n_1 \dot{\gamma} \lambda_i}{\lambda_i} t \quad \text{and} \quad t_{2,i} = \frac{1 + n_2 \dot{\gamma} \lambda_i}{\lambda_i} t$$

**Cessation of Steady - Shear Flow**

$$\eta^-(t, \dot{\gamma}) = \sum_i \left[ \frac{f G_{oi} \lambda_i}{(1 + n_1 \dot{\gamma} \lambda_i)^2} + \frac{(1-f) G_{oi} \lambda_i}{(1 + n_2 \dot{\gamma} \lambda_i)^2} \right] \exp(-t / \lambda_i) \quad (11)$$

$$\psi_1^-(t, \dot{\gamma}) = \sum_i \left[ \frac{2f G_{oi} \lambda_i^2}{(1 + n_1 \dot{\gamma} \lambda_i)^3} + \frac{2(1-f) G_{oi} \lambda_i^2}{(1 + n_2 \dot{\gamma} \lambda_i)^3} \right] \exp(-t / \lambda_i) \quad (12)$$

(a) [Wagner *et al*, 1976 (12)] [Kalyon *et al*, 1988 (13)]

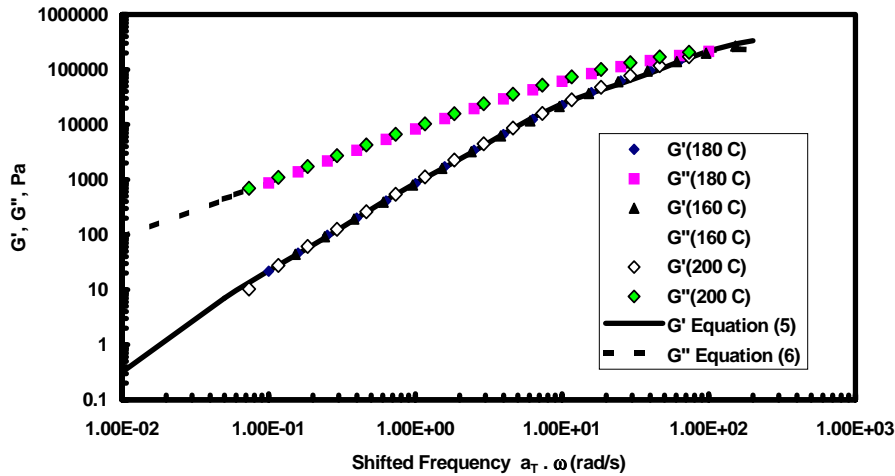


Figure 1. Storage and Loss Moduli of PE - 350 Collected at 160-200 °C and Their Best Fit

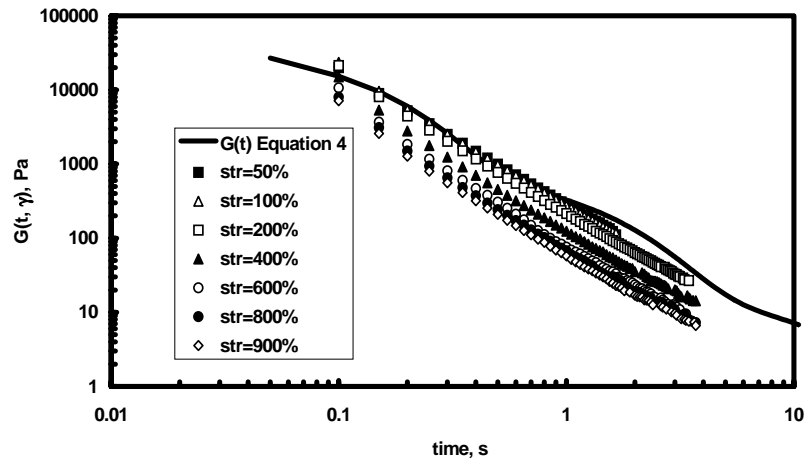


Figure 2 Shear Relaxation Modulus of PE - 350 at 180 °C

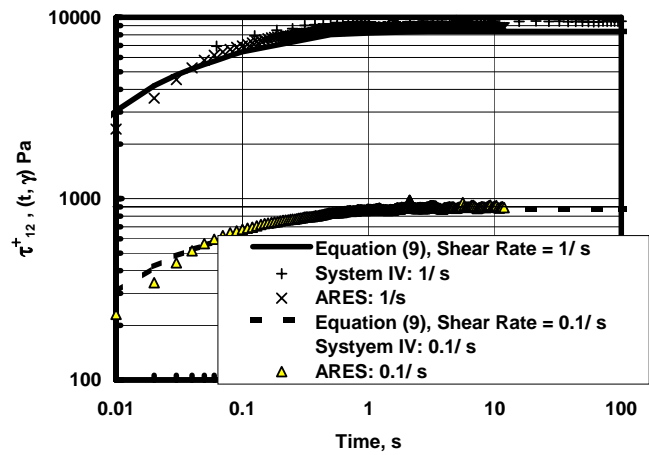


Figure (3) Shear Stress Growth for PE - 350 at 180 °C

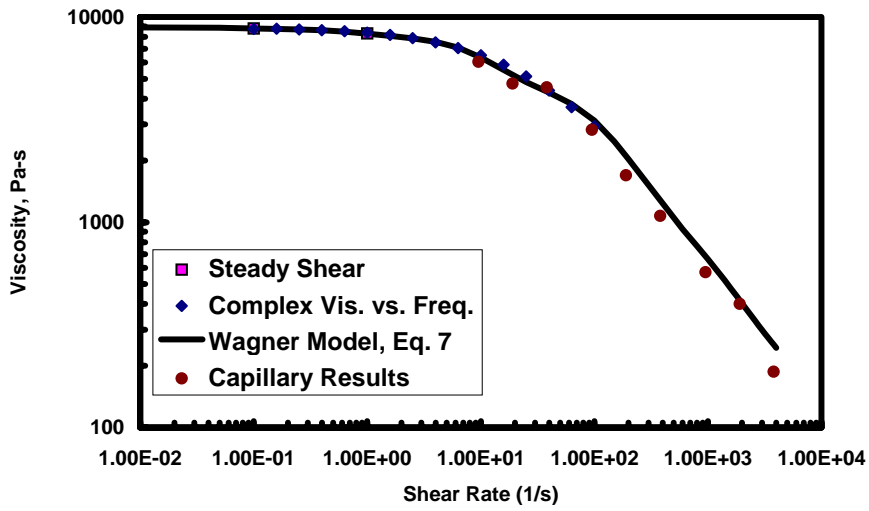


Fig. 4 Viscosity As a Function of Shear Rate at 180°C for PE 350

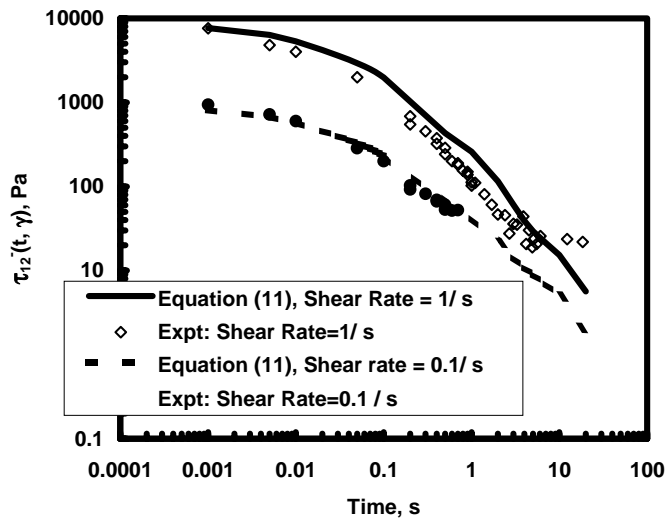


Figure 5 Shear Stress Relaxation Upon the Cessation of Steady Shear for PE - 350 at T = 180°C